Shell model for buoyancy-driven turbulence

Abhishek Kumar* and Mahendra K. Verma†
Department of Physics, Indian Institute of Technology Kanpur, Kanpur 208 016, India
(Received 30 September 2014; revised manuscript received 25 January 2015; published 22 April 2015)

In this paper we present a unified shell model for stably stratified and convective turbulence. Numerical simulation of this model for stably stratified flow shows Bolgiano-Obukhbov scaling in which the kinetic energy spectrum varies as $k^{-11/5}$. The shell model of convective turbulence yields Kolmogorov's spectrum. These results are consistent with the energy flux and energy feed due to buoyancy, and are in good agreement with direct numerical simulations of Kumar *et al.* [Phys. Rev. E **90**, 023016 (2014)].

DOI: 10.1103/PhysRevE.91.043014 PACS number(s): 47.27.te, 47.27.Gs, 47.55.pb

I. INTRODUCTION

Turbulence remains one of the unsolved problems of classical physics. Turbulence generates strong nonlinear interactions among the large number of modes of the system, which makes theoretical analysis of such flows highly intractable. Using Kolmogorov's theory of fluid turbulence, it can be shown that the degrees of freedom of a turbulent flow with Reynolds number Re is $(\mathrm{Re})^{9/4}$ [1]. Consequently, a numerical simulation of a turbulent flow with a moderate Reynolds number of $\mathrm{Re} \approx 10^6$ requires $10^{27/2} \approx 31 \times 10^{12}$ grid points, which is impossible even on the most sophisticated supercomputer of today.

A low-dimensional model called shell model of turbulence [2,3] is reasonably successful in explaining certain features of turbulence, e.g., it reproduces the Kolmogorov's theory of fluid turbulence, as well as the experimentally observed intermittency corrections [2,3]. In a shell model, a single shell represents all the modes of a logarithmically binned shell, hence the number of modes in a shell model is much smaller than $(\mathrm{Re})^{9/4}$. Consequently, a large Reynolds number can be easily achieved in a shell model with 40 or more shells.

A large body of work exists on the shell model of fluid turbulence. However, to date, there is no shell model for the stably stratified turbulence, and there is no convergence on the shell model for the convective turbulence. Brandenburg [4] and Mingshun and Shida [5], have constructed shell models for convective turbulence, namely Rayleigh-Bénard convection, but their results are divergent (to be discussed later; also see Ref. [6]). In this paper, we introduce a shell model that describes both stably stratified and convective turbulence; we can go from one to the other with a change of sign in the density or temperature gradient. Our shell model reproduces the numerical results of Kumar *et al.* [7], according to which stably stratified turbulence exhibits Bolgiano-Obukhov scaling [8–10], and convective turbulence shows Kolmogorov scaling.

Buoyancy-induced turbulence [10], often encountered in geophysics, astrophysics, atmospheric and solar physics, and engineering, come in two categories: (i) Stably stratified flows in which a lighter fluid is above a heavier fluid. These flows are stable because of their stable density stratification; (ii) Convective flows in which a heavier (or colder) fluid is above a lighter (or hotter) fluid. Such flow configurations are unstable, hence, the heavier fluid elements come down, and the lighter ones go up. The linear regimes of the above flow are easy to solve, and they yield gravity waves and convective instabilities respectively. However, the turbulent aspects of such flows are active areas of research.

For stably stratified turbulence, Bolgiano [8] and Obukhov [9] first proposed a phenomenology, according to which for $k < k_B$ (k is wave number, and k_B is Bolgiano wave number [8]), the kinetic energy (KE) spectrum $E_u(k)$, entropy spectrum $E_\theta(k)$, KE energy flux $\Pi_u(k)$, and entropy flux $\Pi_\theta(k)$ are

$$E_u(k) = c_1(\alpha^2 g^2 \epsilon_\theta)^{2/5} k^{-11/5}, \tag{1}$$

$$E_\theta(k) = c_2(\alpha g)^{-2/5} \epsilon_\theta^{4/5} k^{-7/5}, \tag{2}$$

$$\Pi_u(k) = c_3(\alpha^2 g^2 \epsilon_\theta)^{3/5} k^{-4/5}, \tag{3}$$

$$\Pi_\theta(k) = \epsilon_\theta = \text{const.} \tag{4}$$

Here $\mathbf{u}$ and θ are the velocity and temperature fluctuations respectively, α is the thermal expansion coefficient, g is the acceleration due to gravity, ϵ_u and ϵ_θ are the KE and entropy dissipation rates respectively, and $c_i's$ are constants. The KE flux $\Pi_u(k)$ is forward, and it decreases with k due to a conversion of kinetic energy to potential energy. This decrease $\Pi_u(k)$ causes a steepening in the kinetic energy spectrum to $k^{-11/5}$, compared to Kolmogorov's classical $k^{-5/3}$ spectrum. Note that the stably stratified flow is also described in terms of density fluctuation ρ', which leads to an equivalent description since $\rho' \propto -\theta$. In convective turbulence, $\theta^2/2$ is referred to as the entropy, but in stably stratified turbulence, $\rho'^2/2$ is called the potential energy.

Bolgiano [8] also showed that the buoyancy effects become somewhat insignificant in the wave number band $k_B < k < k_d$, where k_d is the dissipation wave number. Therefore, $E_u(k), E_\theta(k) \sim k^{-5/3}$, $\Pi_u(k) = \epsilon_u$, and $\Pi_\theta(k) = \epsilon_\theta$. The aforementioned scaling, $k^{-11/5}$ for $k < k_B$, and $k^{-5/3}$ for $k_B < k < k_d$, is referred to as Bolgiano-Obukhov (BO) phenomenology. For convective turbulence, in particular for the idealized version called Rayleigh-Bénard convection (RBC), Procaccia and Zeitak [11], L'vov [12], L'vov, and Falkovich [13], and Rubinstein [14] argued in favor of BO scaling.

The numerical and experimental findings, however, are inconclusive [10,15–17]. In a recent numerical simulation, Kumar *et al.* [7] analyzed the above phenomenologies in a great detail. They showed that stably stratified turbulence

*abhkr@iitk.ac.in
†mkv@iitk.ac.in

under strong buoyancy exhibits $k^{-11/5}$ energy spectrum, as predicted by Bolgiano [8] and Obukhov [9]. They observed that $F(k) = \mathrm{Re}(\langle u_k \theta_k^* \rangle) < 0$, thus corroborating the net conversion of kinetic energy to potential energy. For RBC, Kumar *et al.* [7] showed that $F(k) = \mathrm{Re}(\langle u_k \theta_k^* \rangle) > 0$, which is interpreted as a conversion of potential energy to kinetic energy, opposite to that in stably stratified turbulence. As a result, for RBC, the KE flux $\Pi_u(k)$ increases marginally with k, and KE exhibits an approximate Kolmogorov spectrum $k^{-5/3}$, contrary to the earlier predictions [11–14]. The numerical results of Kumar *et al.* [7] are consistent with those of Borue and Orszag [18].

The power-law regimes in Kumar *et al.*'s [7] simulations are somewhat narrow. Also, they could not observe the dual spectrum of BO phenomenology, which may require much higher numerical resolution than 1024^3. In this paper, we present a unified shell model of stably stratified and convective turbulence that overcomes some of the aforementioned limitations of the numerical simulations. For the unified shell model for the buoyancy driven flows, we assume that the fluid is subjected to a mean temperature gradient, $d\bar{T}/dz$, which is positive for a stably stratified flow (cold below and hot above), and is negative for a convective flow (hot below and cold above). Here $\bar{T}(z)$ is computed by averaging the temperature over the horizontal plane whose height is at z.

The outline of the paper is as follows. In Sec. II, we introduce unified shell model, which can solve both stably stratified and convective turbulence; we discuss the construction of nonlinear terms, the required constraints, and the method for computing the energy spectrum and flux. Numerical results of the shell models for the stably stratified turbulence and the convective turbulence are discussed in Secs. III and IV, respectively. We conclude in Sec. V.

II. SHELL MODEL FOR BUOYANCY-DRIVEN TURBULENCE

Our shell model for the buoyancy-driven turbulence is

$$\frac{du_n}{dt} = N_n[u,u] + \alpha g \theta_n - \nu k_n^2 u_n + f_n, \tag{5}$$

$$\frac{d\theta_n}{dt} = N_n[u,\theta] - \frac{d\bar{T}}{dz} u_n - \kappa k_n^2 \theta_n, \tag{6}$$

where u_n and θ_n are the shell variables for the velocity and temperature fluctuations respectively, f_n represents the external force field, $k_n = k_0 \lambda^n$ is the wave number of the nth shell, and ν and κ are the kinematic viscosity and thermal diffusivity, respectively, of the fluid. We choose $\lambda = (\sqrt{5}+1)/2$, the golden mean [2].

The nonlinear terms $N_n[u,u]$ and $N_n[u,\theta]$ are constructed keeping in mind the conservation of kinetic energy $\int d\mathbf{r}(u^2/2)$, kinetic helicity $\int d\mathbf{r}(\mathbf{u}\cdot\boldsymbol{\omega})$, and entropy $\int d\mathbf{r}(\theta^2/2)$ in the absence of diffusive and forcing terms. For the shell model, the corresponding qualities are $\sum_n |u_n|^2/2$, $\sum_n (-1)^n k_n |u_n|^2$, and $\sum_n |\theta_n|^2/2$ respectively. The nonlinear term $N_n[u,u]$ has been constructed earlier by invoking the conservation of kinetic energy and kinetic helicity as (see, e.g., Ref. [19])

$$N_n[u,u] = -i(a_1 k_n u_{n+1}^* u_{n+2} + a_2 k_{n-1} u_{n-1}^* u_{n+1} - a_3 k_{n-2} u_{n-1} u_{n-2}) \tag{7}$$

with constraints $a_1 + a_2 + a_3 = 0$ and $a_1 - \lambda a_2 + \lambda^2 a_3 = 0$. For our computation, we choose $a_1 = 1$, $a_2 = \lambda - 2$, and $a_3 = 1 - \lambda$ [2].

For the construction of the nonlinear term $N_n[u,\theta]$, we use the fact that the nonlinear term of the temperature equation is a bilinear product of the temperature fluctuation and the velocity fluctuation. Also, the conservation of entropy yields a condition

$$\mathrm{Re}\left(\sum_n \theta_n^* N_n[u,\theta]\right) = 0. \tag{8}$$

A combination of the above yields

$$N_n[u,\theta] = -i[k_n(d_1 u_{n+1}^* \theta_{n+2} + d_3 \theta_{n+1}^* u_{n+2}) + k_{n-1}(d_2 u_{n-1}^* \theta_{n+1} - d_3 \theta_{n-1}^* u_{n+1}) - k_{n-2}(-d_1 u_{n-1} \theta_{n-2} - d_2 \theta_{n-1} u_{n-2})] \tag{9}$$

with arbitrary d_1, d_2, and d_3. For our shell model, we choose $d_1 = 1$, $d_2 = \lambda - 2$, and $d_3 = 1 - \lambda$. For consistency, we choose the boundary conditions $u_{-1} = u_0 = \theta_{-1} = \theta_0 = 0$ and $u_{N+1} = u_{N+2} = \theta_{N+1} = \theta_{N+2} = 0$, where N is the total number of shells. Also note that we use Sabra model [19] that yields less fluctuations for the spectrum compared to the Gledzer-Ohkitani-Yamada (GOY) model [3,19,20].

The second term in the right-hand side (RHS) of Eq. (5), $\alpha g \theta_n$, is the buoyancy term, while $-(d\bar{T}/dz)$ is the temperature stratification (or equivalently density stratification) term. Clearly, $d\bar{T}/dz > 0$ for a stably stratified flow, and $d\bar{T}/dz < 0$ for the convective turbulence.

The shell model for RBC does not require forcing to maintain a steady state. However, the shell model for the stably stratified turbulence requires a forcing for the same; we force a set of small wave number shells (large length-scale modes) randomly so as to feed a constant energy supply rate ε to the system. We assume that the forcing shells receive an equal amount of energy. If n_f shells are forced, then the above conditions yield the force at the nth shell as

$$f_n = \sqrt{\frac{\varepsilon}{n_f \Delta t}} e^{i\phi_n}, \tag{10}$$

where ϕ_n is the random phase of the nth shell chosen from the uniform distribution in $[0, 2\pi]$. In our simulation we force the shells $n = 3$ and 4, hence $n_f = 2$.

It is convenient to work with the nondimensionalized equations, which is achieved by using box height or the characteristic length d as the length scale, $\sqrt{\alpha g |d\bar{T}/dz| d^2}$ as the velocity scale, and $|d\bar{T}/dz| d$ as the temperature scale. Therefore, $u_n = u_n' \sqrt{\alpha g |d\bar{T}/dz| d^2}$, $\theta_n = \theta_n' |d\bar{T}/dz| d$, $k_n = k_n'/d$, and $t = t'(d/\sqrt{\alpha g |d\bar{T}/dz| d^2})$. In terms of nondimensionalized variables, the equations are

$$\frac{du_n'}{dt'} = N_n'[u',u'] + \theta_n' - \sqrt{\frac{\mathrm{Pr}}{\mathrm{Ra}}} k_n'^2 u_n' + f_n', \tag{11}$$

$$\frac{d\theta_n'}{dt'} = N_n'[u',\theta'] - S u_n' - \frac{1}{\sqrt{\mathrm{RaPr}}} k_n'^2 \theta_n', \tag{12}$$

where $S = 1$ for positive $|d\bar{T}/dz|$, and $S = -1$ for negative $|d\bar{T}/dz|$.

TABLE I. Parameters of our simulations: Flow type [stably stratified turbulence (SST) or convective turbulence (CT)], number of shells N, Rayleigh number Ra, energy supply rate ε, Reynolds number Re, Richardson number Ri, Froude number Fr, kinetic energy dissipation rate ϵ_u, entropy dissipation rate ϵ_θ, and Bolgiano wave number k_B. We choose Pr = 1 for all our runs.

Flow Type	N	Ra	ε	Re	Ri	Fr	ϵ_u	ϵ_θ	k_B
SST1	36	10^5	50	1.0×10^3	0.10	3.2	3.9	3.1	53
SST2	76	10^5	10^{10}	7.9×10^5	1.6×10^{-7}	2.5×10^3	1.4×10^9	7.6×10^3	<1
CT	76	10^{12}	NA	8.7×10^6	0.01	NA	62	60	NA

We remark that ours is a shell model for the stably stratified turbulence. For RBC, Brandenburg [4], and Mingshun and Shida [5] had constructed shell models. Our shell model differs quite significantly from that of Brandenburg. The shell model "2" of Mingshun and Shida [5] is applicable to neutral stratification, and it is a subset of our shell model. The shell model of Ching and Cheng [6] is same as that of Brandenburg [4].

The important parameters for the buoyancy-driven turbulence are the Prandtl number, $\mathrm{Pr} = \nu/\kappa$, the Reynolds number, $\mathrm{Re} = u_{\mathrm{rms}} d/\nu$, and

$$\text{Brunt Väisälä freq. } N_f = \sqrt{\frac{g}{\rho_0}\left|\frac{d\bar{\rho}}{dz}\right|} = \sqrt{\alpha g \left|\frac{d\bar{T}}{dz}\right|}, \quad (13)$$

$$\text{Rayleigh number Ra} = \frac{d^4 \alpha g}{\nu\kappa}\left|\frac{d\bar{T}}{dz}\right|, \quad (14)$$

$$\text{Froude number Fr} = \frac{u_{\mathrm{rms}}}{dN_f}, \quad (15)$$

$$\text{Richardson number Ri} = \frac{\alpha g d^2}{u_{\mathrm{rms}}^2}\left|\frac{d\bar{T}}{dz}\right|, \quad (16)$$

where u_{rms} is the rms velocity of flow, and d is the characteristic length scale. Note that the Brunt-Väisälä frequency is the frequency of the gravity wave, the Froude number is the ratio of the characteristic fluid velocity and the gravitational wave velocity, and the Richardson number is the ratio of the buoyancy and the nonlinearity $(\mathbf{u}\cdot\nabla)\mathbf{u}$. For convenience, the primes from the variables are dropped in our subsequent discussion.

Note that for RBC, the critical Rayleigh number $\mathrm{Ra}_c = 1$, after which the flow becomes unstable. Due to the lower critical Rayleigh number in the shell model, turbulence appears at a lower Rayleigh number compared to that observed in direct numerical simulations. We compute energy spectrum $[E_u(k)]$ and the entropy spectrum $[E_\theta(k)]$, defined as

$$E_u(k) = \frac{|u_k|^2}{k}, \quad (17)$$

$$E_\theta(k) = \frac{|\theta_k|^2}{k}, \quad (18)$$

using the steady-state data.

We also compute the energy and entropy fluxes. In fluid turbulence, the energy flux $\Pi(k)$ is defined [21] as the rate of energy transfer from modes inside a sphere of radius k to the modes outside the sphere. For the shell model, the energy flux $\Pi(k)$ is the rate of energy transfer from the shells within the sphere of radius k, i.e., $m \in [0,k]$, to the shells outside the sphere, i.e., $n \in (k,N]$ [2]:

$$\Pi_u(k) = \sum_{n>k}\sum_{m\leqslant k}\sum_{p} -k_p \mathrm{Im}(u_p u_m u_n^*). \quad (19)$$

Similarly, the entropy flux $\Pi_\theta(k)$ is defined as the rate of entropy transfer from the shells within the sphere of radius k to the shells outside the sphere, i.e.,

$$\Pi_\theta(k) = \sum_{n>k}\sum_{m\leqslant k}\sum_{p} -k_p \mathrm{Im}(u_p \theta_m \theta_n^*). \quad (20)$$

We simulate the aforementioned shell model [Eqs. (11), (12)] for stably stratified and convective turbulence and compute the above spectra and fluxes. We take 36 shells for the stably stratified turbulence simulations SST1 and 76 shells for SST2 and the convective turbulence simulation (CT). For time stepping, we use the fourth-order Runge-Kutta (RK4) method. For stably stratified turbulence, we apply random force on shells $n = 3$ and $n = 4$. The parameters of the simulations are listed in Table I.

We compute the spectra and fluxes of KE and entropy, and average over many snapshots ($\sim 10^8$) of the steady-state flow (of a single run); these values are further averaged over 100 simulations with independent random initial conditions [22,23]. The error bars reported in the paper for the spectral exponents and fluxes are the standard deviations of the aforementioned 100 independent data sets [22,23]. This is the statistical error of our data. The spectral exponents of the energy and entropy spectra along with the errors for the sets of parameters are summarized in Table II. The data also has some systematic error, for example the dip in energy spectrum near $k \approx 7$ (the fifth shell). The origin of the dip is not understood clearly at present, and it will be presented in future.

III. ENERGY AND FLUXES OF STABLY STRATIFIED TURBULENCE

To test the validity of BO scaling in the stably stratified turbulence, we simulate the shell model for the two sets of parameters, SST1 and SST2, which are listed in Table I. In Fig. 1(a) we plot the KE spectrum $E_u(k)$ and entropy spectrum

TABLE II. Spectral exponents of our simulations for the runs SST1, SST2, and CT listed in Table I: KE spectrum $E_u(k) \sim k^{-p}$ and the entropy spectrum $E_\theta(k) \sim k^{-q}$.

Flow Type	p	q
SST1	-2.1677 ± 0.0004	-1.4667 ± 0.0008
SST2	-1.7513 ± 0.0006	-1.6868 ± 0.0007
CT	-1.703 ± 0.003	-1.711 ± 0.003

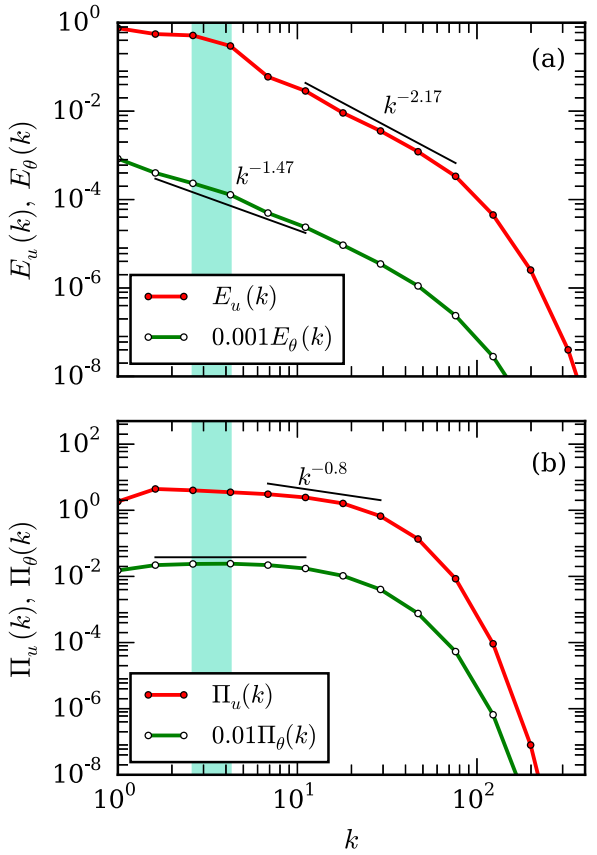

FIG. 1. (Color online) For stably stratified simulation with $\mathrm{Pr} = 1, \mathrm{Ra} = 10^5$, and $\mathrm{Ri} = 0.10$: (a) plots of KE and entropy spectra; (b) plots of KE flux $\Pi_u(k)$ and entropy flux $\Pi_\theta(k)$. The green shaded region shows the forcing range.

$E_\theta(k)$ for $\mathrm{Ra} = 10^5$ and $\mathrm{Ri} = 0.10$. Green shadow regions in all the figures of the paper are the forcing bands. The figure indicates that $E_u(k) \sim k^{-2.17}$ and $E_\theta(k) \sim k^{-1.47}$ for more than a decade, a result consistent with the BO scaling.

We also compute the KE and potential energy fluxes, which are plotted in Fig. 1(b). In the inertial range, the entropy flux $\Pi_\theta(k)$ is constant, and the KE flux $\Pi_u(k)$ decreases with k, but somewhat different from $k^{-4/5}$. These results are in general agreement with the BO scaling for the stably stratified turbulence. We also compute energy supply rate by buoyancy, $F(k) = \mathrm{Re}(\langle u_k \theta_k^* \rangle)$, which is negative, as shown in Fig. 2. Thus, we show a conversion of kinetic energy to potential energy by buoyancy, a result consistent with that of Kumar *et al.* [7].

For the above case, the Bolgiano wave number $k_B \approx 53$, which lies in the dissipation range, thus making the $k^{-5/3}$ KE spectrum inaccessible. The Bolgiano wave number k_B is calculated by comparing Eq. (1) and the Kolmogorov's KE energy spectrum [10]. We also try to investigate the dual spectrum ($k^{-11/5}$ and $k^{-5/3}$) predicted in BO scaling, but increase of Ra shrinks the 11/5 regime and makes it invisible. Dual spectrum requires further search, which is our future plan.

For the parameters of SST2, the nonlinearity is stronger than the buoyancy term, which is evident from the fact the Richardson number $\mathrm{Ri} \ll 1$. Hence, we observe Kolmogorov

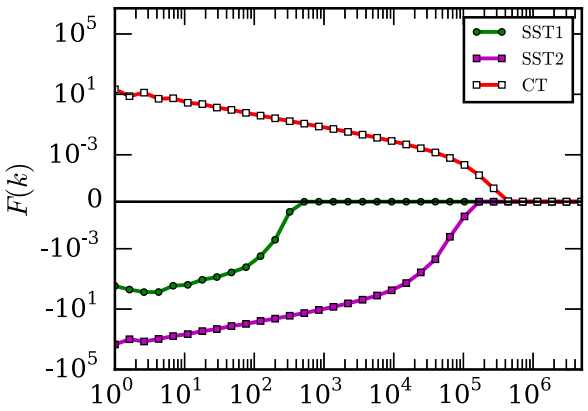

FIG. 2. (Color online) (a) Plots of $F(k)$ for stably stratified turbulence SST1, SST2, and for convective turbulence (CT); $F(k) < 0$ for SST's, but $F(k) > 0$ for CT.

scaling, i.e., $E_u(k) \sim k^{-5/3}$ and $E_\theta(k) \sim k^{-5/3}$ for these parameters shown in Fig. 3(a). The fluxes of KE and potential energy are constant in k, as shown in Fig. 3(b).

In the next section we will discuss the results of convective turbulence.

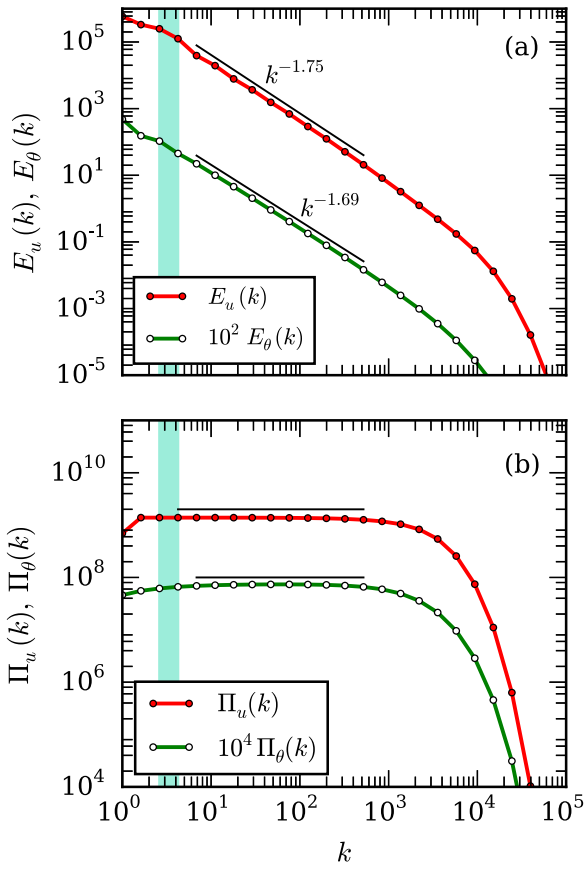

FIG. 3. (Color online) For stably stratified simulation with $\mathrm{Pr} = 1$, $\mathrm{Ra} = 10^5$, and $\mathrm{Ri} = 1.6 \times 10^{-7}$: the (a) plots of KE and entropy spectra; and (b) plots of KE flux $\Pi_u(k)$ and entropy flux $\Pi_\theta(k)$ exhibit Kolmogorov's spectrum since Ri or buoyancy is small.

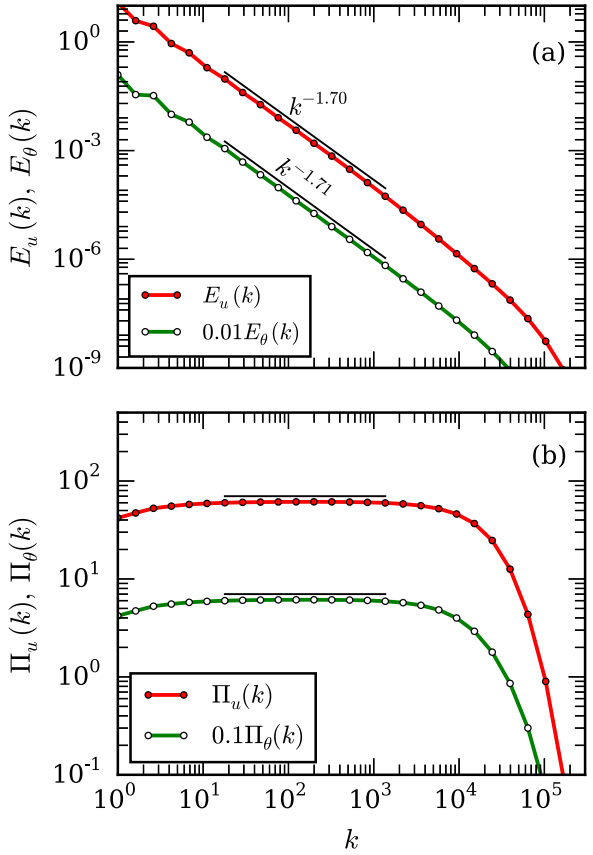

FIG. 4. (Color online) For convective turbulence simulation with $\mathrm{Pr} = 1$ and $\mathrm{Ra} = 10^{12}$, the (a) plots of KE and entropy spectra; (b) plots of KE flux $\Pi_u(k)$ and entropy flux $\Pi_\theta(k)$ exhibit Kolmogorov's spectrum.

IV. ENERGY AND FLUXES OF CONVECTIVE TURBULENCE

In convective turbulence, buoyancy feeds energy to the kinetic energy, hence the KE flux increases marginally at lower wave numbers [7]. In the intermediate range of wave numbers, where the dissipation rate $D(k) = \sum_k 2\nu k^2 |u_k|^2/2$ approximately balances the energy supplied by buoyancy $F(k)$, we expect Kolmogorov's spectrum for the velocity field [7]. We performed a shell model simulation to verify the above conjecture using the parameters $\mathrm{Pr} = 1$ and $\mathrm{Ra} = 10^{12}$ (CT of Table I). Note that no external forcing is required to obtain a steady state in convective turbulence.

In Fig. 4(a) we plot the KE and entropy spectra that indicates Kolmogorov (KO) scaling, i.e., $E_u(k) \sim k^{-5/3}$ and $E_\theta(k) \sim k^{-5/3}$, for convective turbulence. Our spectrum results are consistent with the KE and entropy fluxes computations, which are plotted in Fig. 4(b). The KE flux $\Pi_u(k)$ and entropy flux $\Pi_\theta(k)$ are constant in the inertial range, $20 < k < 1000$. We also compute energy supply rate $F(k) = \mathrm{Re}(\langle u_k \theta_k^* \rangle)$ and plot it in Figs. 2 and 5. We observe that $F(k) > 0$ indicating a positive energy transfer from buoyancy to the kinetic energy. In Fig. 5, we also plot the dissipation rate $D(k)$ and $F(k) - D(k)$. In inertial range, $F(k)$ and $D(k)$ cancel each other approximately, and hence yield a constant KE flux $\Pi_u(k)$.

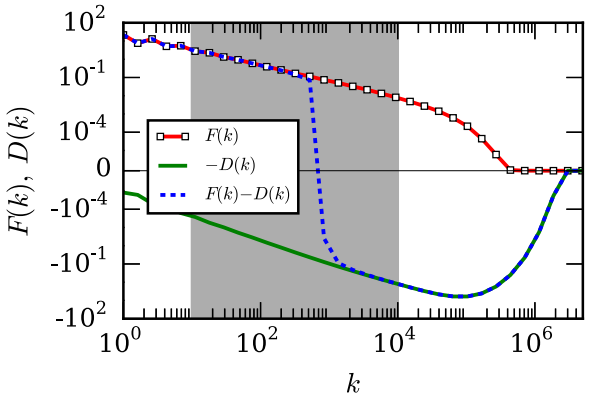

FIG. 5. (Color online) For RBC run (CT), plots of $F(k)$, $-D(k)$, and $F(k) - D(k)$ for CT; the shaded region where $F(k) \approx D(k)$ is the inertial range.

Thus, we show that in convective turbulence, the KE exhibits Kolmogorov's spectrum, not BO spectrum, as envisaged in some of the earlier work [11–14].

V. DISCUSSIONS AND CONCLUSIONS

It is important to contrast our shell model with earlier ones. Ours is the first shell model for stably stratified turbulence, and it yields results consistent with the BO scaling predicted by Bolgiano [8] and Obukhov [9].

By switching the sign of the density gradient, our shell model transforms from stably stratified flows to convective turbulence. For convective turbulence, our shell model exhibits Kolmogorov's spectrum in the intermediate range of wave numbers. Earlier, Brandenburg [4] and Mingshun and Shida [5] had constructed shell models for RBC. Brandenburg's [4] shell model is quite different from ours; he added several new terms in the GOY shell model, which leads to both forward and inverse KE fluxes. He observes $E_u(k) \sim k^{-5/3}$ for the forward cascade regime, consistent with our model. However, an inverse cascade of KE flux yields $E_u(k) \sim k^{-11/5}$, which is consistent with the flux arguments of Kumar *et al.* [7]. When $\Pi_u(k) < 0$ and $F(k) > 0$, Eq. (26) of Kumar *et al.* [7] would yield $|\Pi_u(k + \Delta k)| < |\Pi_u(k)|$, which could possibly yield $|\Pi_u(k)| \sim k^{-4/5}$ (BO scaling). These arguments need a clear-cut validation from numerical simulations. Ching and Cheng [6] used Brandenburg's shell model and studied multiscaling exponents.

The shell model "2" of Mingshun and Shida [5] is applicable to neutral stratification, and it is a subset of our shell model. Mingshun and Shida [5] reported Kolmogorov's spectrum for the model 2, hence our model is consistent with the shell model of Mingshun and Shida [5].

We also remark that the shell models are applicable to three-dimensional isotropic turbulence. The numerical work of Kumar *et al.* [7] focuses on Froude number of the order of unity that yields somewhat isotropic flow. This is the reason why our shell model is consistent with the numerical results of Kumar *et al.* [7]. However, our present shell model is not expected to work for anisotropic stably stratified flows studied earlier for which the Froude number is quite low [24,25]. A

modification of our shell model to two-dimensional flows may work for the aforementioned quasi-two-dimensional systems.

In summary, we constructed a unified shell model for the buoyancy driven turbulence that yields BO scaling for stably stratified flows, but Kolmogorov's spectrum for convective turbulence. Such low-dimensional models have strong utility since they can be used to explore highly nonlinear regimes, which are inaccessible to numerical simulations and experiments.

ACKNOWLEDGMENTS

We thank Sagar Chakraborty for valuable suggestions, and Pankaj Mishra for performing initial set of numerical simulations. Our numerical simulations were performed at HPC2013 and Chaos clusters of IIT Kanpur. This work was supported by a research grant (Grant No. SERB/F/3279) from Science and Engineering Research Board, India.

[1] U. Frisch, *Turbulence: The Legacy of A N Kolmogorov* (Cambridge University Press, Cambridge, 2011).
[2] P. Ditlevsen, *Turbulence and Shell Models* (Cambridge University Press, Cambridge, 2011).
[3] L. Biferale, Ann. Rev. Fluid Mech. **35**, 441 (2003).
[4] A. Brandenburg, Phys. Rev. Lett. **69**, 605 (1992).
[5] J. Mingshun and L. Shida, Phys. Rev. E **56**, 441 (1997).
[6] E. S. C. Ching and W. C. Cheng, Phys. Rev. E **77**, 015303 (2008).
[7] A. Kumar, A. G. Chatterjee, and M. K. Verma, Phys. Rev. E **90**, 023016 (2014).
[8] R. Bolgiano, J. Geophys. Res. **64**, 2226 (1959).
[9] A. N. Obukhov, Dokl. Akad. Nauk SSSR **125**, 1246 (1959).
[10] D. Lohse and K. Q. Xia, Ann. Rev. Fluid Mech. **42**, 335 (2010).
[11] I. Procaccia and R. Zeitak, Phys. Rev. Lett. **62**, 2128 (1989).
[12] V. S. L'vov, Phys. Rev. Lett. **67**, 687 (1991).
[13] V. S. L'vov and G. E. Falkovich, Physica D **57**, 85 (1992).
[14] R. Rubinstein, NASA Technical Memorandum 1066602 (1994).
[15] J. J. Niemela, L. Skrbek, K. R. Sreenivasan, and R. J. Donnelly, Nature (London) **404**, 837 (2000).
[16] J. Zhang, X. L. Wu, and K. Q. Xia, Phys. Rev. Lett. **94**, 174503 (2005).
[17] P. K. Mishra and M. K. Verma, Phys. Rev. E **81**, 056316 (2010).
[18] V. Borue and S. A. Orszag, J. Sci. Comput. **12**, 305 (1997).
[19] V. S. L'vov, E. Podivilov, A. Pomyalov, I. Procaccia, and D. Vandembroucq, Phys. Rev. E **58**, 1811 (1998).
[20] E. Gledzer, Sov. Phys. Dokl. **18**, 216 (1973); K. Ohkitani and M. Yamada, Prog. Theor. Phys. **81**, 329 (1989).
[21] M. K. Verma, Phys. Rep. **401**, 229 (2004).
[22] S. S. Ray, D. Mitra, and R. Pandit, New J. Phys. **10**, 033003 (2008).
[23] S. Chakraborty, M. H. Jensen, and A. Sarkar, Eur. Phys. J. B **73**, 447 (2010).
[24] E. Lindborg, J. Fluid Mech. **550**, 207 (2006).
[25] A. Vallgren, E. Deusebio, and E. Lindborg, Phys. Rev. Lett. **107**, 268501 (2011).